Implementation of the SP_3 equations in a MOOSE-based application

Roberto E. Fairhurst Agosta, Kathryn D. Huff

University of Illinois at Urbana-Champaign, Dept. of Nuclear, Plasma, and Radiological Engineering
ref3@illinois.edu

INTRODUCTION

This work presents the implementation of the Simplified P_3 (SP_3) equations [1] in a Multi-physics Object-Oriented Simulation Environment (MOOSE)-based application. MOOSE [2] is a computational framework that supports engineering analysis applications. In a nuclear reactor, several partial differential equations describe its physical behavior. These equations are typically nonlinear, and they are often coupled to each other. MOOSE is an open-source Finite Element Method (FEM) framework that supports the development of applications for solving such systems.

All the software built on the MOOSE framework shares the same Application Programming Interface (API), facilitating relatively easy coupling between different phenomena. While the SP_3 equations solve the neutronics in a nuclear reactor, other applications may solve the thermal-fluids, and given they share the same API; their integration is straightforward.

The P_N method [3] discretizes the transport equation by expanding the angular dependence of the neutron flux in spherical harmonics, considering up to order N polynomials. If $N \to \infty$, the solution of the P_N equations tends to the exact transport solution. In three-dimensional geometries, the number of P_N equations is proportional to $(N+1)^2$, whereas, in one-dimensional planar geometries, the number of P_N equations is $(N+1)$. Gelbard [1] proposed the SP_N approximation by replacing the second derivatives in the one-dimensional planar P_N equations with three-dimensional Laplacian operators. This approximation considerably reduces the number of equations conserving a reasonable accuracy. Capilla et al. [4] studied a modified version of the C5 Mixed-Oxide (MOX) fuel Benchmark [5] introduced by Brantley and Larsen [6] comparing the P_3 and SP_3 methods, the difference between results being less than 40 pcm.

The SP_N approximation has the disadvantage that the solution does not usually converge to the true transport solution as $N \to \infty$. Additionally, the theoretical basis of Gelbard's formulation of SP_N approximation was weak. For these reasons, the method did not gain widespread use until the 2000s, when thanks to Pomraning [7], Brantley, and Larsen's [6] contribution, the method gained a stronger theoretical basis.

In practice, the SP_N equations are most accurate for diffusive problems or for problems in which the solution behaves nearly one-dimensionally and has weak tangential derivatives at material interfaces. For problems with strong, multidimensional transport effects, such as voids, streaming regions, or geometrically complex regions, the SP_N solutions are less accurate [8]. However, several results show that the SP_N approximation yields more accurate solutions than the diffusion approximation [9] [10] [11] [12] [13] with considerably less computational expense than the discrete ordinates (S_N) method [6]. For example, the SP_3 approximation is preferable over the diffusion approximation for modeling reactors using MOX/UO_2 fuel assemblies. MOX fuel assemblies have higher thermal absorption and fission cross-sections than UO_2 fuel assemblies, and consequently, their thermal flux is lower while their power production higher. Modeling these characteristics using the diffusion approximation may be challenging [6] [4].

The SP_3 approximation gained usage throughout the last couple of decades and currently, different software uses it to solve the neutron transport equation. Some of those software are PARCS [8], DYN3D [10], and COCAGNE [11].

METHODOLOGY

This section describes the methodology followed for solving the equations. Davidson [3] defined the one-dimensional multi-group P_N equations. For $N = 3$ and steady-state, the equations become

$$\frac{d}{dx}\phi_{1,g} + \Sigma_{t,g}\phi_{0,g} = \sum_{g'=1}^{G}\Sigma_{s0,g'\to g}\phi_{0,g'} + \frac{\chi_g}{k_{eff}}\sum_{g'=1}^{G}\nu\Sigma_{f,g'}\phi_{0,g'} + Q_{0,g} \quad (1)$$

$$\frac{1}{3}\frac{d}{dx}\phi_{0,g} + \frac{2}{3}\frac{d}{dx}\phi_{2,g} + \Sigma_{t,g}\phi_{1,g} = \sum_{g'=1}^{G}\Sigma_{s1,g'\to g}\phi_{1,g'} + Q_{1,g} \quad (2)$$

$$\frac{2}{5}\frac{d}{dx}\phi_{1,g} + \frac{3}{5}\frac{d}{dx}\phi_{3,g} + \Sigma_{t,g}\phi_{2,g} = \sum_{g'=1}^{G}\Sigma_{s2,g'\to g}\phi_{2,g'} + Q_{2,g} \quad (3)$$

$$\frac{3}{7}\frac{d}{dx}\phi_{2,g} + \Sigma_{t,g}\phi_{3,g} = \sum_{g'=1}^{G}\Sigma_{s3,g'\to g}\phi_{3,g'} + Q_{3,g} \quad (4)$$

where

$\phi_{n,g} = n^{th}$ moment of group g neutron flux
$\Sigma_{t,g}$ = group g macroscopic total cross-section
$\Sigma_{sn,g'\to g} = n^{th}$ moment of the group g' to group g macroscopic scattering cross-section
$\nu\Sigma_{f,g}$ = group g macroscopic production cross-section
χ_g = group g fission spectrum
k_{eff} = eigenvalue
$Q_{n,g} = n^{th}$ moment of group g external neutron source
G = number of energy groups.

Assuming an isotropic external source and negligible anisotropic group-to-group scattering [6]

$$Q_{n,g} = 0, \quad n > 0$$
$$\Sigma_{sn,g'\to g} = 0, \quad g' \neq g, \quad n > 0$$

simplifies equations 2 and 4, allowing to express the odd moments of the flux $\phi_{1,g}$ and $\phi_{3,g}$ as functions of the even moments $\phi_{0,g}$ and $\phi_{2,g}$. Introducing $\phi_{1,g}$ and $\phi_{3,g}$ into equations 1 and 3 reduces the system from four to two equations. Introducing the variables $\Phi_{0,g}$ and $\Phi_{2,g}$, reorganizing the equations, and replacing the second derivatives by Laplacian operators [1] yields the SP_3 equations [10]

$$-D_{0,g}\Delta\Phi_{0,g} + \Sigma_{0,g}\Phi_{0,g} - 2\Sigma_{0,g}\Phi_{2,g} = S_{0,g} \tag{5}$$

$$-D_{2,g}\Delta\Phi_{2,g} + \left(\Sigma_{2,g} + \frac{4}{5}\Sigma_{0,g}\right)\Phi_{2,g} - \frac{2}{5}\Sigma_{0,g}\Phi_{0,g} = -\frac{2}{5}S_{0,g} \tag{6}$$

where

$$\begin{aligned}
\Sigma_{n,g} &= \Sigma_{t,g} - \Sigma_{sn,g'\to g} \\
\Phi_{0,g} &= \phi_{0,g} + 2\phi_{2,g} \\
\Phi_{2,g} &= \phi_{2,g} \\
D_{0,g} &= \frac{1}{3\Sigma_{1,g}} \\
D_{2,g} &= \frac{9}{35\Sigma_{3,g}} \\
S_{0,g} &= \sum_{g'\neq g}^{G} \Sigma_{s0,g'\to g}\left(\Phi_{0,g'} - 2\Phi_{2,g'}\right) \\
&\quad + \frac{\chi_g}{k_{eff}} \sum_{g'=1}^{G} \nu\Sigma_{f,g'}\left(\Phi_{0,g'} - 2\Phi_{2,g'}\right) + Q_{0,g}.
\end{aligned} \tag{7}$$

The Marshak-like vacuum boundary conditions (BCs) complete the system of equations [10]

$$\frac{1}{4}\Phi_{0,g} \pm \frac{1}{2}\hat{n}\cdot J_{0,g} - \frac{3}{16}\Phi_{2,g} = 0 \tag{8}$$

$$-\frac{3}{80}\Phi_{0,g} \pm \frac{1}{2}\hat{n}\cdot J_{2,g} + \frac{21}{80}\Phi_{2,g} = 0 \tag{9}$$

where

$$J_{n,g} = -D_{n,g}\nabla\Phi_{n,g}.$$

Finally, multiplying equations 5 and 6 by a test function and integrating over the domain yields the weak form of the equations modularized into kernels in the MOOSE-based application. For brevity, we will not display the derivation of the kernels here. Such procedure is standard in weighted residual methods and can be found in [12] and any finite elements book [14].

RESULTS

This section presents several numerical results that validate the calculation scheme. The following sections discuss the results of a one group exercise presented in [6] and describe the results of the C5 MOX Benchmark [5].

One group two-dimensional problem

This section describes a one group, isotropic-scattering eigenvalue problem introduced by Brantley and Larsen [6]. This section also presents the eigenvalue obtained with the SP_3 solver and compares it against the reference value. Figure 1 shows the problem's geometry, and Table I specifies its cross-sections. Due to the problem's symmetry, the model included only a quarter of the core. We created the mesh using the *Gmsh* [15] meshing tool. The mesh had 6×10^3 elements. The simulation convergence criterion was 10^{-8} for the neutron flux.

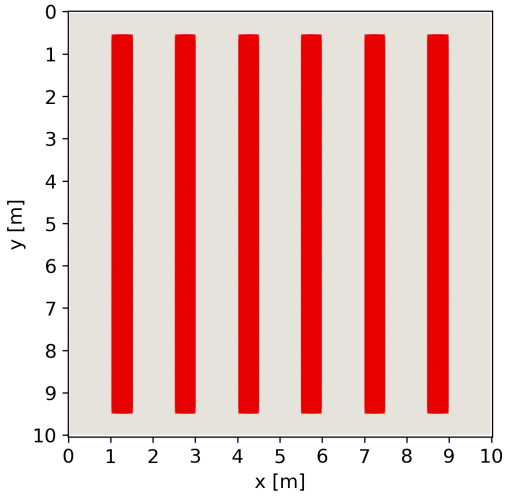

Fig. 1: Geometry of the one group eigenvalue problem. Fuel in red. Moderator in gray.

Material	Σ_t	Σ_{s0}	$\nu\Sigma_f$
Moderator	1.00	0.93	0.00
Fuel	1.50	1.35	0.24

TABLE I: Cross-sections of the one group eigenvalue problem [6]. Values expressed in cm^{-1}.

Table II compares the eigenvalue obtained with the SP_3 solver and the reference value [6] using the equation

$$\Delta_\rho = \left|\frac{k_{SP_3} - k_{Ref}}{k_{SP_3}k_{Ref}}\right| \tag{10}$$

where

Δ_ρ = reactivity difference $[pcm]$
k_{SP_3} = eigenvalue obtained with SP_3 solver
k_{Ref} = reference eigenvalue.

C5 MOX Benchmark

This section introduces the C5 MOX Benchmark [5] and presents the SP_3 solver results. The Organisation for Economic Co-operation and Development (OECD)/Nuclear Energy Agency (NEA) developed this benchmark to validate

k_{Ref}	k_{SP_3}	Δ_ρ
0.79862	0.79854	12

TABLE II: Comparison between the result obtained with the SP_3 solver and the reference result for the one group eigenvalue problem.

methods and identify their strengths, limitations, and accuracy, and suggest needs for method development. Two types of fuel assembly (MOX and UO_2) and a reflector comprise the core, shown in Figure 2. Each fuel assembly consists of a 17×17 array of squared pin cells, as displayed in Figures 3 and 4. The dimensions of each pin cell are 1.26×1.26 cm, being 21.42 $\times$ 21.42 cm the dimensions of each assembly, and 128.52 $\times$ 128.52 cm of the whole core. The benchmark [5] specifies the cross-sections, which have a two-energy group structure.

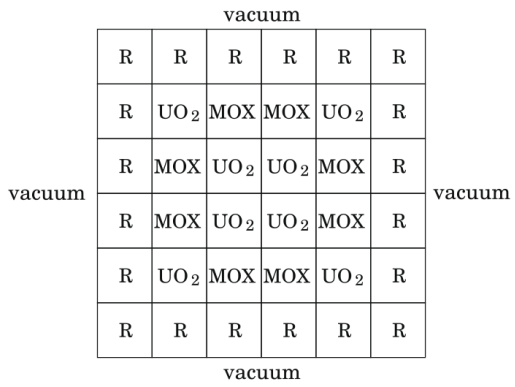

Fig. 2: C5 MOX benchmark configuration. R correponds to the reflector region. Image reproduced from [4].

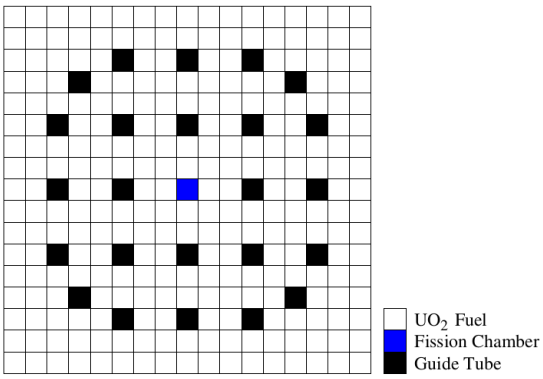

Fig. 3: Structure of the UO_2 assembly. Image reproduced from [4].

When no anisotropic component of the scattering cross-section is available, the benchmark recommends applying the diagonal transport correction

$$D_{0,g} = \frac{1}{3\Sigma_{tr,g}} \qquad (11)$$
$$\Sigma_{tr} = \Sigma_{t,g} - \bar{\mu}_g \Sigma_{s0,g}$$

where

$\Sigma_{tr,g}$ = group g transport cross-section

$\bar{\mu}_g$ = group g average cosine deviation angle.

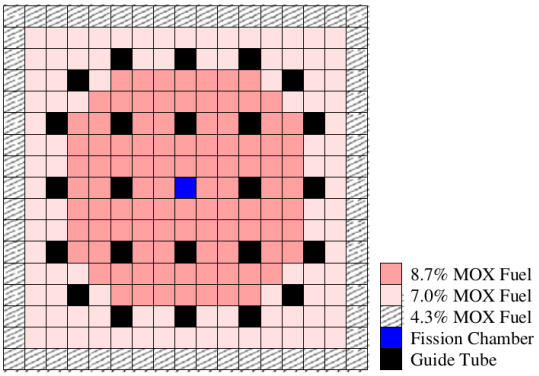

Fig. 4: Structure of the MOX assembly. Image reproduced from [4].

For the sake of comparison, we conducted the exercise with and without the transport correction for calculating $D_{0,g}$ with equations 11 and 7, respectively. Due to the problem's symmetry, the model included only a quarter of the core. The mesh had 2.4×10^4 elements. The simulation convergence criterion was 10^{-8} for the neutron flux.

Table III compares the eigenvalues obtained with the SP_3 solver and the references. For the method without correction, we used an eigenvalue reference value from Capilla et al. [4] as they conducted the exercise without correction. For the method with transport correction, we used the reference value from the benchmark [5].

	k_{Ref}	k_{SP_3}	Δ_ρ
No correction	0.96969	0.97106	145
Transport correction	0.93755	0.93792	43

TABLE III: Comparison between the results obtained with the SP_3 solver using no correction (equation 7), the transport correction (equation 11), and the reference results for the C5 MOX Benchmark.

The results obtained with the SP_3 solver are within 145 pcm of the reference values. However, the difference between the reference values of the different schemes is 3535 pcm, suggesting that the use of the transport correction is necessary.

Figure 5 presents the power distribution and the relative difference to the reference provided by the benchmark [5]. For conciseness, we only calculated the power distribution using the transport correction. The benchmark specifies the power distribution pin-by-pin, but to simplify displaying the results, Figure 5 presents the power distribution in each assembly. The results of the power distribution are within the 1% difference.

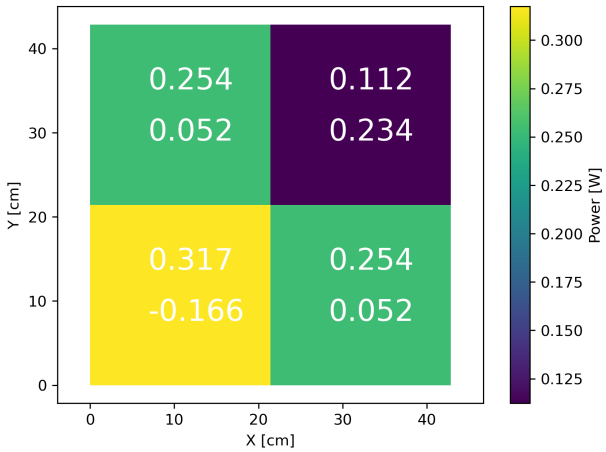

Fig. 5: Power distribution in the C5 MOX Benchmark. Top: power distribution. Bottom: relative difference to reference values expressed in %.

CONCLUSIONS

MOOSE is a computational framework that solves systems of nonlinear differential equations. As part of this work, we implemented the kernels to solve the steady-state SP_3 equations in a MOOSE-based application. Additionally, we carried out two exercises whose reference results were known. The first exercise solved a one-group eigenvalue problem with a simple geometry, with a result within the 12 pcm. The second exercise studied the C5 MOX Benchmark, solving it using different approaches and obtaining results within the 145 pcm. The calculated power distribution values were within the 1% error from the reference.

While the SP_3 equations solve the neutronics in a nuclear reactor, future work may develop other applications to solve the thermal-fluids or integrate this application to existing applications. MOOSE-based applications share the same API making their integration straightforward.

ACKNOWLEDGEMENTS

This research is being performed using funding received from the DOE Office of Nuclear Energy's University Program (Project 20-19693, DE-NE0008972) 'Evaluation of microreactor requirements and performance in an existing well-characterized micro-grid'. Prof. Huff is also supported by the Nuclear Regulatory Commission Faculty Development Program (award NRC-HQ-84-14-G-0054 Program B), the Blue Waters sustained-petascale computing project supported by the National Science Foundation (awards OCI-0725070 and ACI-1238993) and the state of Illinois, the DOE ARPA-E MEITNER Program (award DE-AR0000983), and the DOE H2@Scale Program (Award Number: DE-EE0008832).

REFERENCES

1. E. GELBARD, "Application of spherical harmonics methods to reactor problems," Technical Report WAPD-BT-20, Bettis Atomic Power Laboratory (1960).
2. D. GASTON, C. NEWMAN, G. HANSEN, and D. LEBRUN-GRANDIÉ, "MOOSE: A parallel computational framework for coupled systems of nonlinear equations," *Nuclear Engineering and Design*, **239**, *10*, 1768–1778 (Oct. 2009).
3. B. DAVIDSON, *Neutron Transport Theory*, Oxford University Press, London (1957).
4. M. CAPILLA, D. GINESTAR, and G. VERDÚ, "Applications of the multidimensional equations to complex fuel assembly problems," *Annals of Nuclear Energy*, **36**, *10*, 1624–1634 (Oct. 2009).
5. C. CAVAREC, J. PERRON, D. VERWAERDE, and J. WEST, "Benchmark Calculations of Power Distributions within Assemblies," Technical Report HT-12/94006 A, NEA/NSC/DOC (94) 28, Nuclear Energy Agency Committee on Reactor Physics (1994).
6. P. BRANTLEY and E. LARSEN, "The Simplified P3 Approximation," *Nuclear Science and Engineering* (2000).
7. G. POMRANING, "Asymptotic and variational derivations of the simplified PN equations," *Annals of Nuclear Energy*, **20**, *9*, 623–637 (Sep. 1993).
8. T. DOWNAR, D. LEE, Y. XU, and T. KOZLOWSKI, "PARCS v2.6 US NRC Core Neutronics Simulator THEORY MANUAL," Technical Report, School of Nuclear Engineering Purdue University, W. Lafayette, Indiana (Jun. 2004).
9. A. MUI, Y. KIM, and D. HARRIS, "Modified P3 transport improvements for reactor diffusion calculations," Transactions of the American Nuclear Society, Los Angeles, CA, USA (Nov. 1987), vol. 55, pp. 584–586.
10. C. BECKERT and U. GRUNDMANN, "Development and verification of a nodal approach for solving the multigroup SP3 equations," *Annals of Nuclear Energy* (2007).
11. M. FLISCOUNAKIS, E. GIRARDI, T. COURAU, and D. COUYRAS, "Potential of pin-by-pin SPN calculations as an industrial reference," in "ICAPP Proceedings," Chicago, USA (Jun. 2012).
12. E. H. RYU and H. G. JOO, "Finite element method solution of the simplified P3 equations for general geometry applications," *Annals of Nuclear Energy*, **56**, 194–207 (Jun. 2013).
13. M. KHOSRAVI MIRZAEE, A. ZOLFAGHARI, and A. MINUCHEHR, "Reactor core analysis through the SP3-ACMFD approach. Part I: Static solution," *Nuclear Engineering and Technology*, **52**, *2*, 223–229 (Jul. 2019).
14. A. QUARTERONI and A. VALLI, *Numerical Approximation of Partial Differential Equations*, no. 23 in Springer Series in Computational Mathematics, Springer-Verlag, Berlin, Heidelberg (1994).
15. C. GEUZAINE and J.-F. REMACLE, "Gmsh: a three-dimensional finite element mesh generator with built-in pre- and post-processing facilities." *International Journal for Numerical Methods in Engineering* (2009).